Journal of Alloys and Compounds 509 (2011) 10179–10184

Contents lists available at SciVerse ScienceDirect

Journal of Alloys and Compounds

journal homepage: www.elsevier.com/locate/jallcom

Microstructure characterization and tensile properties of β phase containing TiAl pancake

H.Z. Niu*, F.T. Kong, Y.Y. Chen, F. Yang

School of Materials Science and Engineering, Harbin Institute of Technology, P.O. Box 434, Harbin 150001, PR China

ARTICLE INFO

Article history:
Received 3 July 2011
Received in revised form 13 August 2011
Accepted 17 August 2011
Available online 31 August 2011

Keywords:
Intermetallics
Forging
Microstructure
Tensile properties

ABSTRACT

The microstructure and tensile properties of Ti–44Al–6V–3Nb–0.3Y (at.%) alloy after canned forging were investigated. SEM results showed that the TiAl pancake exhibits inhomogeneous microstructure, which can be ascribed to the temperature drop and friction between billet and outer pack during forging, as well as the intrinsic anisotropy of lamellar colony. By means of TEM observation and EBSD analysis, the microstructure in the dominant area of the pancake was further characterized. This deformation area consists of 87.7% content of γ grains plus some refined lamellar colonies and the rest of B2 grains. The grain size ranges between 1 μm and 8.5 μm. High-angle boundaries dominate the deformation microstructure, several substructures and twins are observed as well. Additionally, current forged alloy exhibits excellent high temperature tensile strength and noteworthy yield stress anomaly (YSA), with ultimate tensile strength 680 MPa and yield strength 620 MPa at room temperature, increasing to 850 MPa and 750 MPa at 700 °C, respectively. The anomalous strengthening of current TiAl alloy is temperature dependent and can be interpreted by the dislocation cross-slip pinning mechanism.

1. Introduction

TiAl based alloys are highly promising for high-temperature structural applications in aerospace and automotive industries, due to their attractive properties, such as low density, good elevated temperature strength, high resistance to oxidation, excellent creep properties [1,2]. However, the low room temperature ductility and poor deformability limit their extensive applications [2–4]. One of the best means to improve the ductility of TiAl alloys is to convert the coarse grained, textured and segregated microstructure into a more homogenous and fine grained microstructure through alloying [5], heat treatment [6], thermo-mechanical treatment (TMT) [7–10], including isothermal forging, pack-forging, hot extrusion and rolling etc. Recently, β phase containing TiAl alloys have been developed widely, due to their excellent hot deformability and refined microstructure by β solidification [8,11–13]. However, previous researches indicated that coarse β phase existing in TiAl alloys deteriorates creep resistance and room temperature properties [14,15].

TiAl ingot generally has a dominant coarse lamellar microstructure. It is nearly impossible to completely break down the lamellar microstructure through thermo-mechanical processing [16,17]. Thus the wrought microstructure generally consists of fine-grained recrystallized areas plus some remnant lamellar colonies. Hot processing techniques, process variables and the initial microstructures determine the resulting amount of remnant lamellar colonies and the final homogenization degree [17,18]. The nonuniform deformation microstructure with coarse residual lamellar colonies will lead to deformation incompatibility and flow localization during subsequent hot rolling or forming process and deteriorate the mechanical properties of finished products [18–20]. Therefore, how to eliminate the remnant lamellar structure and ensure the deformation microstructure homogeneous is an important matter necessary to be considered during processing of TiAl alloys.

In this study, the microstructure of as-forged Ti–44Al–6V–3Nb–0.3Y (at.%) pancake was characterized comprehensively, by means of SEM, TEM and EBSD techniques. And the reason for the nonuniform deformation microstructure was discussed in detail. Furthermore, the tensile properties at room temperature, 700 °C and 800 °C were tested; the anomalous hardening phenomenon of this as-forged alloy was interpreted as well.

2. Experimental procedure

The ingot with a nominal composition of Ti–44Al–6V–3Nb–0.3Y (at.%) was prepared by induction skull melting (ISM) in a water-cooled copper crucible. An ingot with dimensions of approximately Φ120 mm × 220 mm was gained, then was hot isostatic pressed (HIPed) at 1200 °C for 4 h under a pressure of 140 MPa and aged at 900 °C for 48 h. Cylindrical billet (Φ90 mm × 100 mm) was cut from ingot by electric-discharge machining and then canned by 20 mm thick steel pack. A pancake with

* Corresponding author. Tel.: +86 451 86418802; fax: +86 451 86418802.
E-mail address: hzniu@126.com (H.Z. Niu).

0925-8388/$ – see front matter. Crown Copyright © 2011 Published by Elsevier B.V. All rights reserved.
doi:10.1016/j.jallcom.2011.08.078

Fig. 1. The can-forged Ti–44Al–6V–3Nb–0.3Y alloy pancake.

dimensions of Φ170 mm × 20 mm (Fig. 1) was obtained by two-step canned forging conducted at 1200 °C and 0.01 s^{-1}, using an engineering strain of 80%.

The microstructures were characterized by scanning electron microscopy (SEM) in back-scattered electron (BSE) mode, transmission electron microscopy (TEM) and Electron Back scattered Diffraction (EBSD) techniques. TEM sample was cut from the core area, thin TEM foils were prepared by mechanical polishing and twin-jet electropolishing using a solution of 6% perchloric acid + 34% butanol + 60% methanol at −20 °C and 25 V. The EBSD sample was cut close to the core of pancake perpendicular to forging direction, and then prepared using the same process as TEM samples, except that the electropolishing time was 15 s. The data collection was conducted at intervals of 0.3 μm and the collected EBSD data were treated with TSL OIM Analysis software.

Flat tensile samples were cut from the central area of the pancake, all the tensile tests were conducted on Instron universal test machine at room temperature, 700 °C and 800 °C, driven at crosshead speed of 0.5 mm min^{-1}.

3. Results and discussion

3.1. Nonuniform deformation microstructure

Fig. 2 shows the deformation microstructures in different sampling points in the as-received TiAl pancake. As shown in Fig. 2(a), the core area features a fully dynamic recrystallization (DRX) microstructure consisting of fine equiaxed grains. The black areas indicate γ phase and the bright represent B2 (ordered β phase), which can be confirmed by subsequent EBSD analysis. Some coarse and elongated residual lamellar colonies appear in Fig. 2(b), which means that the DRX did not proceed completely near the surface area in the center. From Fig. 2(c)–(e), it can be clearly seen that the microstructures at the sampling points of 0.25 r and 0.5 r are characterized by dominated fine DRX grains plus some refined lamellar colonies. Similar to the microstructure shown in Fig. 2(b), an incompletely DRX microstructure with dominant coarse and elongated lamellar colonies can be observed near the edge area in Fig. 2(f), dynamic recrystallization preferentially took place along lamellar colony boundaries.

The fully or nearly fully dynamic recrystallization district in forged pancake is generally called "large deformation zone", while the partly dynamic recrystallization district, such as the edge and surface of the pancake, is called "difficult deformation zone". The microstructure difference between the two areas can be ascribed to inhomogeneous plastic flow during canned forging. Usually, heat loss and the resulting temperature drop during forging are inevitable, especially at the ends of the billet. According to Wang's research on heat loss during pack forging of TiAl alloys [21], temperature drop at the ends of the billet is expected to be 100 °C more than on the surface, because effects of heat transfer by steel subplates are more significant than surface radiation effects during hot forging. Meanwhile, the temperature of the billet can be raised by plastic deformation and internal friction. Consequently, a large temperature gradient generates in the billet, and the core area has much higher temperature. As well known, plastic deformation is a typically thermally activated process, during forging, the deformation or dynamic recrystallization preferentially proceeds in the central zone of the billet, and the strain (plastic flow) decreases gradually from center to edge (or surface). Additionally, for current β solidified TiAl alloy, transformation $\alpha \rightarrow \gamma$+B2 readily takes place under the condition of hot forging, as soon as the temperature decreases slightly lower than 1200 °C. The α laths decomposition and B2 phase generation further facilitate the dynamic recrystallization, especially in the core of the TiAl billet. DRX and large strain make the dominant central area even softer by breaking down the coarse lamellar colonies, in turn, inducing more subsequent deformation, which finally results in a completely DRX area in the central area, while a partly DRX area near the surface and edge of the pancake. Furthermore, the friction between pack and bullet is also unavoidable during forging, which, together with temperature drop, causes stress concentration and difficult plastic flow zone near the boundary between the outer pack and TiAl billet, especially at the ends of the billet. Overall, the temperature drop and friction during forging are primary causes to bring about incompletely DRX and give rise to coarse residual lamellar colonies. Wang et al. [21] have reported that deformation uniformity degree can be improved by optimizing the pack thickness and using thermal insulation at the ends of the billet.

Note that in Fig. 2(b) and (f), the interfaces of the residual lamellar colonies are approximately perpendicular to the forging direction. This can be interpreted by the anisotropic plastic flow features of lamellar colonies. Inui et al. [22], reported that the yield stress of lamellar colonies strongly depends on the orientation angle Φ between lamellar boundaries and loading axis. According to calculation on PST TiAl at 1100 °C, the yield stress is the highest (about 260 MPa) when the orientation angle Φ is 90°. This is a hard orientation, the deformation can only shear along lamellar interfaces and α phase will deform in its hardest slip mode. During pack forging, the coarse lamellar colonies were elongated and bended by dislocation slip at first, and dynamic recrystallization would proceed in some soft-orientated lamellar colonies and along grain boundaries. While the effective strain was not enough to arouse completely dynamic recrystallization in the coarse hard-orientated lamellar colonies, resulting in an incomplete DRX area with some residual lamellar colonies at last. This interpretation is consistent with the investigations on forged TiAl [17], and extruded TiAl [23], that the interfaces of the residual lamellar colonies are perpendicular to the forging or extrusion direction. In short, the inhomogeneous deformation microstructures of current TiAl pancake are mainly caused by nonuniform plastic flow, which are induced by both external factors including temperature drop and friction during forging, and intrinsic anisotropy of coarse lamellar colonies.

As discussed above, the large deformation zone, i.e. the completely DRX areas such as Fig. 2(a), (c) and (d), dominates the current pancake. This dominant zone exhibits relatively fine and uniform DRX microstructures. In addition, TiAl plates for subsequent pack rolling of TiAl sheet are generally cut from this zone. Therefore, it is necessary to characterize the microstructures and study the properties of the large deformation zone.

3.2. Microstructure characterization of the large deformation zone

The bright-field TEM images in Fig. 3 reveal the subtle microstructures of the TiAl pancake. From Fig. 3(a), some

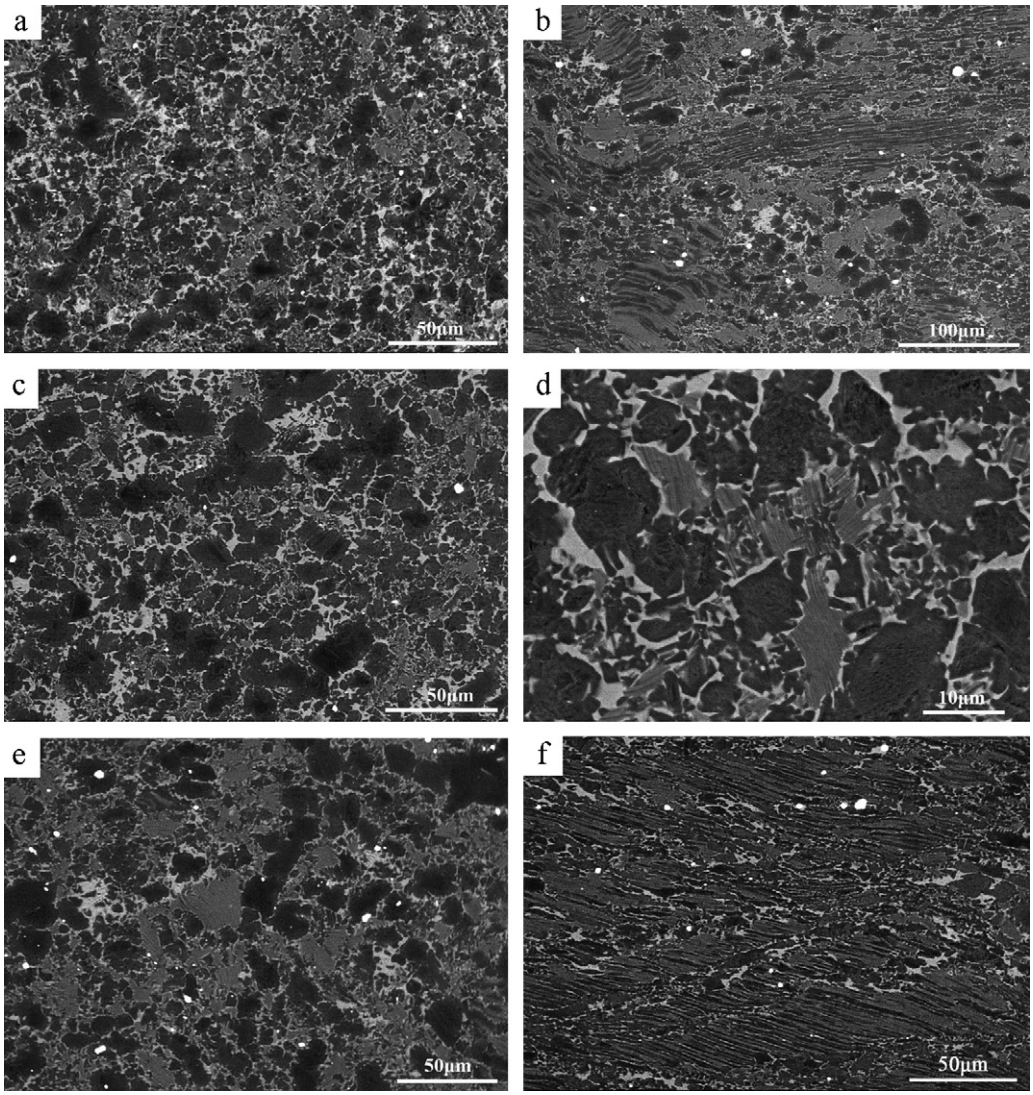

Fig. 2. BSE images showing microstructures in different sampling points of the forged pancake. (a) near core (b) near surface in the center, (c) 0.25 r, (d) high magnification image of (c), (e) 0.5 r and (f) near edge. For image (b) and (f), the forging direction is vertical. For images (c)–(f), samples were cut along horizontal center plane of the pancake.

dislocation-free statically recrystallized γ grains are observed in the crooked lamellar colony. This residual lamellar colony displays high density of dislocations, and the statically recrystallized γ grains are generally induced by dislocation recovery, due to the high stored energy in lamellae during forging. Fig. 3(b) shows the twins intersection in γ grain. Moreover, fine DRX grains can be clearly seen in Fig. 3(c). As known, the plastic deformation of γ-TiAl takes place by either dislocation slip or mechanical twins. Slip generally proceeds by four ordinary dislocations of $1/2\langle 1\,1\,0\rangle\{1\,1\,1\}$, eight super dislocations of $\langle 1\,0\,1\rangle\{1\,1\,1\}$ and four twinning systems $1/6\langle 11\bar{2}\rangle\{111\}$ [24], and only the $1/6\langle 11\bar{2}\rangle\{111\}$ slip systems do not change the ordered $L1_0$ structure. During forging, multiple slip systems were operated, thereby dynamic recrystallization could proceed almost completely and several twins generated in the large deformation zone, as shown in Figs. 2 and 3.

Fig. 4 presents an EBSD phase map overlaid with low (1°–15°) and high (15°–180°) angle boundaries. As shown, the microstructure consists of dominant γ (87.7%) and a few B2 (11.4%) grains. Almost no α (α_2) phase is found, mainly because the α laths in lamellar colony cannot be detected by EBSD using current scanning step of 0.3 μm. Meanwhile, combined with the SEM results in Fig. 2, the EBSD phase result confirms that the DRX areas are composed of equiaxed γ and B2 grains, and several refined lamellar colonies. Moreover, the DRX microstructure features predominant high-angle boundaries (77.1% content) and 22.9% low-angle boundaries (red color). The detailed distribution of boundary misorientation angles is represented in Fig. 5(a). We can clear see a relatively high content of small misorientation angles (lower than 5°) and a peak value of 90°. As is well known, high angle boundaries are generally caused by dynamic recrystallization and grains growing up through swallowing up or merging, while low angle boundaries are normally the features of substructures generating during forging. Noteworthy that, subgrains with high-angle boundaries mainly exist in DRX γ grains or refined residual lamellar colonies, these subgrains readily grew up from substructures with low-angle boundaries during forging and contributed to further breaking down the coarse grains, especially the residual lamellar colonies, through dynamic recrystallization. Because coarse lamellar colonies generally accumulated higher dislocation density and stored energy during hot forging. Fig. 5(b) reveals the grain size distribution of DRX area shown in Fig. 4. Overall, the DRX grain size is no larger than 8.5 μm, and for half content of the DRX grains, the grain size is between 1 μm and 4 μm. The coarse casting microstructure of the TiAl alloy has been effectively broken down by dynamic recrystallization during hot forging.

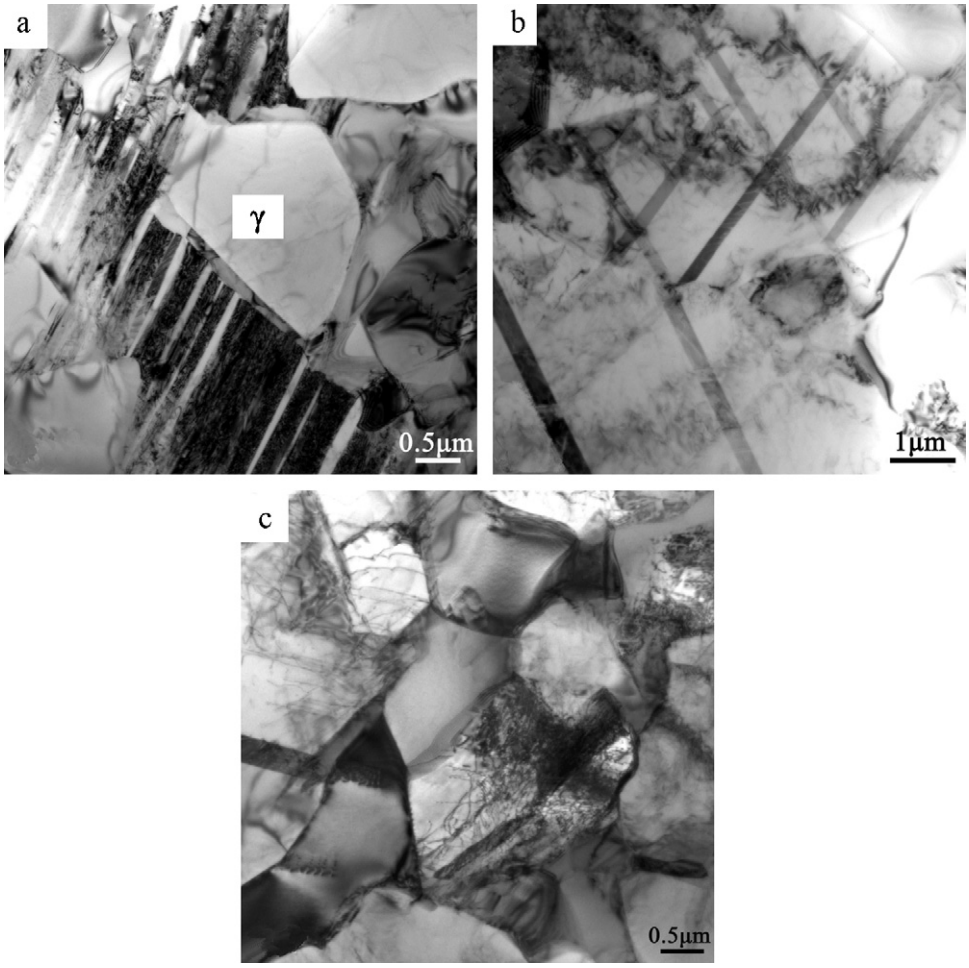

Fig. 3. Bright-field TEM images showing microstructures of pancake. (a) statically recrystallized γ grains in residual lamellar colony, (b) twins and (c) dynamically recrystallized grain.

3.3. *Tensile properties of current forged TiAl alloy*

Tensile properties of as-forged Ti–44Al–6V–3Nb–0.3Y alloy are shown in Fig. 6. At room temperature (RT), the yield strength (YS) and ultimate strength (UTS) of current forged alloy are 620 MPa and 680 MPa respectively, with an elongation (δ) of 0.95%. While testing at 700 °C, the YS, UTS and δ values increase to 710 MPa, 850 MPa and 31.5%, respectively. As discussed above, the central zone of current forged TiAl is characterized by dominant fine DRX grains with grains size no more than 8.5 μm. According to

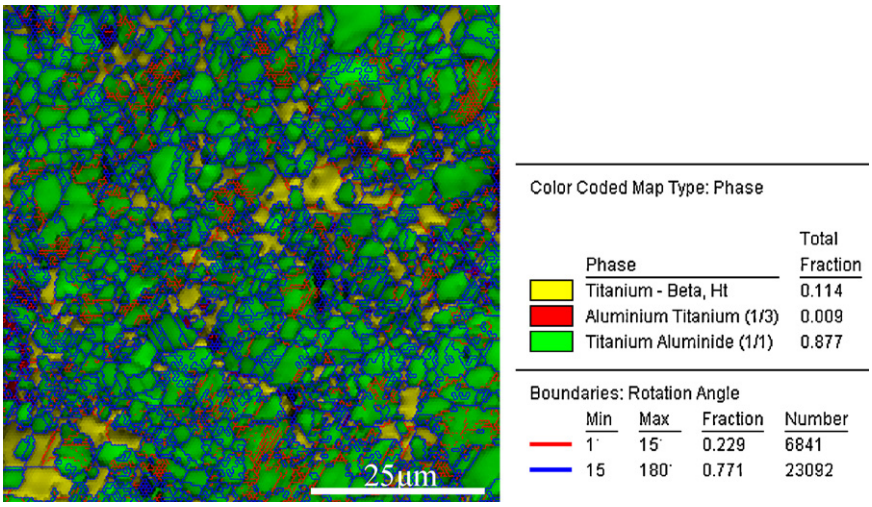

Fig. 4. The EBSD phase map overlaid with low and high angle boundaries.

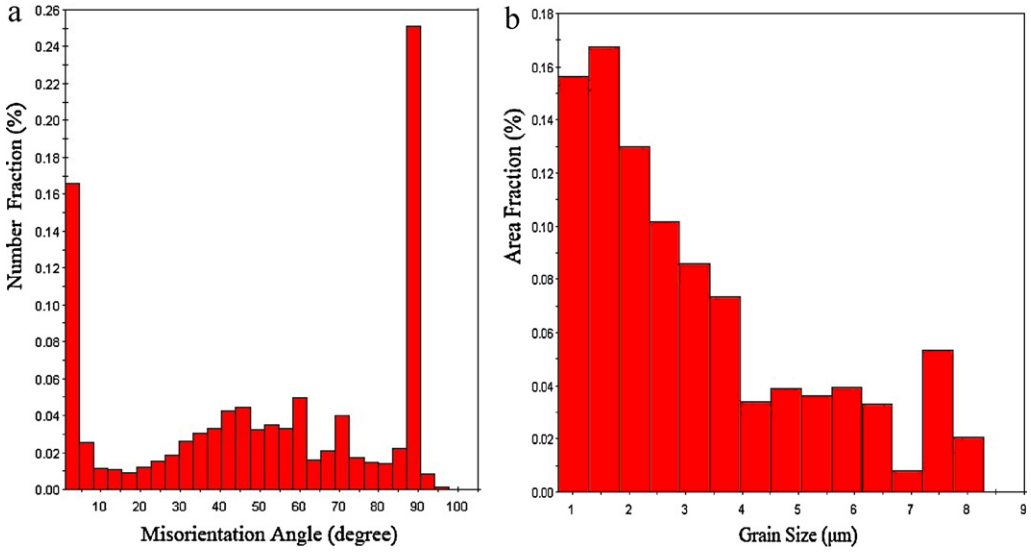

Fig. 5. The EBSD charts presenting distribution of (a) misorientation angle, (b) grain size.

Hall–Petch equation, $\sigma_s = \sigma_o + kd^{-1/2}$, the fine DRX grain size is beneficial to the RT tensile strength, as well as both the RT and elevated temperature ductility, but to the elevated temperature strength. Meanwhile, as well-known, the high density of dislocations (Fig. 3), substructures and mechanical twins (Figs. 3 and 4) contribute to strengthening TiAl alloys, but lower the ductility. That is why the alloy has relatively lower elongation ($\delta = 0.95\%$) at RT. The existence of B2 grains in TiAl alloy is found detrimental to both RT ductility and high temperature strength [14]. However, the tensile yield strength at 700 °C is 90 MPa higher than that at RT, i.e. the tensile yield stress increases with increasing the temperature. This is so-called "yield stress anomaly" (YSA). By now, the generally accepted mechanism for "YSA" in intermetallic compounds is the thermally activated cross-slip of dislocations and the resulting dislocation locking (Kear-Wilsdorf locks) [25,26]. Generally, the two dominant slip systems for plastic deformation and anomalous hardening in TiAl alloys are ⟨1 1 0]{1 1 1} ordinary slip and ⟨1 0 1]{1 1 1} superdislocation slip. Ordinary dislocations in deformed γ-TiAl are rarely observed at relatively low temperature, but they become more active with temperature increasing, particularly above 700 K–1073 K [27,28]. Ordinary dislocations in γ-TiAl frequently crosswise slip onto various non-primary slip planes, inducing the dislocation locking and anomalous yield stress.

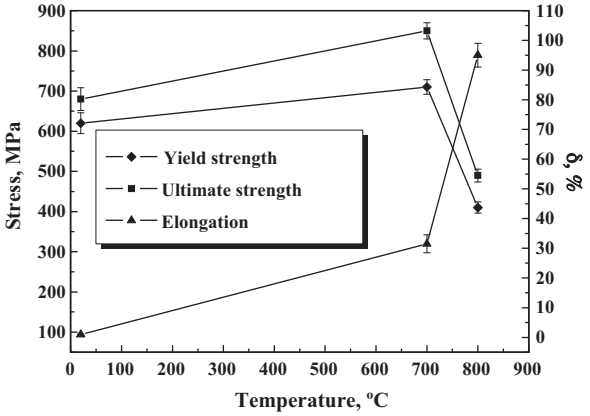

Fig. 6. Tensile properties of as-forged Ti–44Al–6V–3Nb–0.3Y alloy.

Whereas the ⟨1 0 1]{1 1 1} superdislocation slip more easily starts at relatively moderate temperatures, due to its lower CRSS (Critical Resolved Shear Stress) than that of ordinary dislocation slip. During deformation, dissociation and pinning of the ⟨1 0 1] superdislocation can take place to induce the dislocation dipole, also leading to the anomalous yield strength in the YSA temperature domain.

By contrast, when testing temperature exceeds the YSA domain, the crystal lattice will be softened and the dislocation locks can be unlocked. Consequently, the YSA phenomenon disappears when it is easier for dislocations to slip and the grain boundaries to slide, due to the intense thermal activation effect with temperature increasing. At 800 °C, for example, without the YSA phenomenon, current TiAl alloy exhibits lower YS (410 MPa) and UTS (490 MPa) than those obtained at RT and 700 °C. Meanwhile, note that in Fig. 6, the tensile superplasticity is nearly achieved at 800 °C, with an elongation (δ) of 95%, which can be mainly ascribed to the fine DRX microstructures and the soft bcc B2 phase. In short, the anomalous hardening (YS and UTS) and further normally softening of current TiAl alloy are temperature dependent, which can be called "cross-slip pinning and unzipping" process.

4. Conclusions

The main conclusions arising from this study of microstructures and tensile properties of the can-forged Ti–44Al–6V–3Nb–0.3Y alloy are as follows.

(1) The can-forged Ti–44Al–6V–3Nb–0.3Y (at.%) pancake exhibits inhomogeneous microstructures, with plentiful residual lamellar colonies existing in the edge and surface areas. The nonuniform microstructures can be ascribed to the ununiform plastic flow during forging, which is caused by temperature drop and the friction between billet and outer pack, together with the intrinsic anisotropy of lamellar colony.
(2) The deformation microstructure of current alloy is characterized by dominant DRX γ grains and 11.4% content of B2 grains, α_2 phase only exists in refined lamellar colonies. The grain size is between 1 μm and 8.5 μm. Moreover, the DRX microstructures feature mainly high angle boundaries, several deformation substructures and twins are observed as well.

(3) Current forged alloy exhibits excellent high temperature tensile strength and obvious yield stress anomaly (YSA), with an ultimate tensile strength 680 MPa and yield strength 620 MPa at RT, increasing to 850 MPa and 750 MPa at 700 °C, respectively. The dislocation cross-slip pinning mechanism can be used to account for the current anomalous hardening phenomenon.

Acknowledgement

This work was financially supported by the National Natural Science Foundation of China under grant 51074058.

References

[1] Y.W. Kim, Mater. Sci. Eng. A192/193 (1995) 519–533.
[2] X.H. Wu, Intermetallics 14 (2006) 1114–1122.
[3] Y.W. Kim, JOM 47 (1995) 39–41.
[4] Y.W. Kim, Trans. Nonferrous Met. Soc. China 9 (1999) 298–308.
[5] R.M. Imayev, V.M. Imayev, M. Oehring, F. Appel, Intermetallics 15 (2007) 451–460.
[6] H. Clemens, A. Bartels, S. Bystrzanowski, H. Chladil, Intermetallics 14 (2006) 1380–1385.
[7] T. Tetsui, S. Shindo, S. Kobayashi, M. Takeyama, Intermetallics 11 (2003) 299–306.
[8] T. Tetsui, S. Shindo, S. Kaji, S. Kobayashi, M. Takeyama, Intermetallics 13 (2005) 971–978.
[9] S.L. Draper, D. Krause, B. Lerch, I.E. Locci, B. Doehnert, Mater. Sci. Eng. A464 (2007) 330–342.
[10] T. Carneiro, Y.W. Kim, Intermetallics 13 (2005) 1000–1007.
[11] H. Clemen, B. Boeck, W. Wallgram, Mater. Res. Soc. Symp. Proc. 1128 (2009) 3–6.
[12] Y.G. Jin, J.N. Wang, J. Yang, Y. Wang, Scripta Mater. 51 (2004) 113–117.
[13] B.H. Li, Y.Y. Chen, J. Alloys Compd. 473 (2009) 123–126.
[14] G. Chen, W. Zhang, Y. Wang, G. Wang, Z. Sun, in: R. Darolia, J.J. Lewandowski, C.T. Liu, P.L. Martin, D.B. Miracle, M.V. Nathal (Eds.), Structural Intermetallics, TMS, Warrendale, PA, 1993, pp. 319–324.
[15] A.M. Hodge, L.M. Hsiung, T.G. Nieh, Scripta Mater. 51 (2004) 411–415.
[16] P.L. Martin, D.A. Hardwick, D.R. Clemens, W.A. Konkel, M.A. Stucke, in: M.V. Nathal, et al. (Eds.), Structural Intermetallics, TMS, Warrendale, PA, 1997, p. 387.
[17] D.L. Anton, in: M.V. Nathal, et al. (Eds.), Structural Intermetallics, TMS, Warrendale, PA, 1997, p. 269.
[18] S.L. Semiatin, J.C. Chesnutt, C. Austin, V. Seetharaman, in: M.V. Nathal, et al. (Eds.), Structural Intermetallics, TMS, Warrendale, PA, 1997, p. 263.
[19] S.L. Semiatin, V. Seetharaman, I. Weiss, Mater. Sci. Eng. 243 (1998) 1–24.
[20] H. Clemens, W. Glatz, N. Eberhardt, H.-P. Martinz, W. Knabl, in: C. Koch, C.T. Liu, N. Stoloff, A. Wanner (Eds.), High-Temperature Intermetallic Alloys VII, vol. 460, MRS, 1997, p. 29.
[21] L. Wang, Y. Liu, W. Zhang, H. Wang, Q. Li, Intermetallics 19 (2011) 68–74.
[22] H. Inui, K. Kishid, M. Misaki, M. Kobayashi, Y. Shirai, M. Yamaguchi, Philos. Mag. A7 (1995) 1609–1631.
[23] W.J. Zhang, U. Lorenz, F. Appel, Acta Mater. 48 (2000) 2803–2813.
[24] W.T. Marketz, F.T. Fischer, H. Clemens, Int. J. Plast. 19 (2003) 281–321.
[25] F.R.N. Nabarro (Ed.), Dislocations in Solids, vol. 10, Elsevier, Amsterdam, 1996.
[26] B.A. Grinberg, M.A. Ivanov, Intermetallic compounds Ni_3Al and TiAl: Microstructure and Deformation Behavior, Ural Division of the Russian Academy of Sciences, Yekaterinburg, 2002 (in Russian).
[27] Q. Feng, S.H. Whang, Intermetallics 7 (1999) 971–979.
[28] Z. Jiao, S.H. Whang, M.H. Yoo, Q. Feng, Mater. Sci. Eng. A329–A331 (2002) 171–176.